Induced spiral motion in cardiac tissue due to alternans

Taylor Cameron and Jörn Davidsen*

Complexity Science Group, Department of Physics and Astronomy, University of Calgary, Calgary, Alberta T2N 1N4, Canada

(Received 4 October 2012; published 17 December 2012)

Spiral wave meander is a typical feature observed in cardiac tissue and in excitable media in general. Here, we show for a simple model of excitable cardiac tissue that a transition to alternans—a beat-to-beat temporal alternation in the duration of cardiac excitation—can also induce a transition in the spiral core motion that is related to the presence of synchronization defect lines (SDLs) or nodal lines. While this is similar to what has been predicted and indeed observed for complex-oscillatory media close to onset, we find important qualitative differences. For example, single straight SDLs rotate and induce an additional nonresonant frequency characterizing the core motion of the attached spiral. We analyze this behavior quantitatively as a function of the steepness of the restitution curve and show that the velocity and the directionality of the core motion vary monotonically with the control parameter. Our findings agree with recent observations in rat heart tissue cultures indicating that the described behavior is of rather general nature. In particular, it could play an important role in the context of potentially life-threatening cardiac arrhythmias such as fibrillation for which alternans and spiral waves are known precursors.

DOI: 10.1103/PhysRevE.86.061908 PACS number(s): 87.19.Hh, 89.75.Kd, 05.45.Xt

I. INTRODUCTION

Rotating spiral waves in (quasi-) two-dimensional reaction-diffusion systems with local excitable or simple oscillatory dynamics have been investigated extensively both theoretically and experimentally because of their relevance for a variety of physical, chemical, and biological processes [1–3]. One particular feature of spiral waves in excitable media is that they can undergo core instabilities [4]. The classic example is the meander instability, which leads to flowerlike tip trajectories [5–7]. While this instability is well understood theoretically, this is not the case for other instabilities of spiral waves in excitable media. Progress in this direction is crucial since spirals—called reentries in the cardiac context—are known to play a key role in the genesis of abnormally rapid life-threatening heart rhythm disorders [8,9].

Recently, it was found that spiral waves in *in vitro* tissue cultures of neonatal rat ventricular myocytes can undergo an instability such that the spirals exhibit alternans behavior [10]. Alternans is an oscillation in the duration of the action potential (AP) or pulse duration such that short and long APs alternate while the average period remains constant. This behavior typically occurs when the time interval between subsequent APs is sufficiently short and it has been extensively studied in the context of paced cables and tissue (see Refs. [11–13] and references therein). While alternans is widely acknowledged as a precursor of the development of cardiac fibrillation, leading to sudden cardiac death [14–16], its occurrence in and interaction with spiral waves, corresponding to tachycardia, remains largely unexplored.

Spiral waves exhibiting alternans or period-two behavior in general have not only been observed in excitable media but were indeed first reported in complex-oscillatory media [3,17–19]. One generic feature of any period-two spiral waves is the existence of synchronization defect lines (SDLs) or nodal lines. These correspond to points in the medium where the dynamics is locally period 1 and each SDL separates domains of different oscillation phases. Spirals with attached SDLs were first observed in numerical model studies of complex-oscillatory media [17] and subsequently in experiments on the Belousov-Zhabotinsky reaction in a comparable regime [20–25]. The bifurcation from a regular or period-one spiral to a period-two spiral was later put on a solid mathematical foundation by Sandstede *et al.* [26] and identified as a 2 : 1 resonant Hopf bifurcation for models of complex-oscillatory media. One of the important implications of their analytical findings is that period-two spirals drift with a finite velocity. This induced ballistic motion of the spiral core and its implications for multispiral patterns were studied in detail in Ref. [27]. In particular, it was found for the Rössler model, a paradigmatic model for complex-oscillatory media, that the drift velocity increases as a power law from onset and that the direction of the drift is determined by the SDLs attached to the core. Close to onset the angle between the direction of the drift and the straight SDLs is 180 degrees and this angle decreases monotonically to a minimum of about 90 degrees far from onset.

Motivated by the above-mentioned experimental observation of spirals exhibiting alternans behavior in rat heart tissue cultures [10], recent theoretical investigations have started to focus on period-two spirals and SDLs in models of excitable cardiac tissue [13,28,29]. While some questions related to the number of SDLs attached to a spiral [28] and the shape of SDLs [13] have already been addressed, this is not the case for the motion of period-two spirals in such systems. Here, we address exactly this open problem focusing especially on spirals with single SDLs attached to them. For a simple conceptual model of excitable cardiac tissue, we find that the transition from period-one to period-two spirals also induces a meandering transition in the core motion but with nonresonant features. The second frequency characterizing the meandering motion is much smaller than the spiral frequency leading to inward petals. Moreover, the drift velocity associated with this

*davidsen@phas.ucalgary.ca

second frequency increases monotonically from onset and is directed at a well-defined angle from the SDL, which rotates with the same frequency. Interestingly, the angle increases monotonically from onset which is opposite to what has been observed for the Rössler model.

II. MODEL

To investigate the motion of period-two spirals, we consider a simple model of excitable cardiac tissue first proposed in Ref. [30]. This model has been shown to exhibit stationary discordant alternans under periodic pacing as well as period-two spirals with SDLs [28]. An advantage of this model is that for weakly excitable parameter regimes the spirals do not have to be pinned in order to have a *single* SDL attached to them. We focus on this case here in order to perform a direct comparison with the experimental findings of Ref. [10] for cardiac tissue, and models of complex-oscillatory media [27], both of which observe spirals with single SDLs attached to the cores.

The model equations are based on the standard wave equations for cardiac tissue and can be written in the following form,

$$\frac{\partial E}{\partial t} = \gamma \Delta E + \tau_E^{-1} f(E,n), \tag{1}$$

$$\frac{\partial n}{\partial t} = \tau_n^{-1} g(E,n), \tag{2}$$

where the two variables E and n, refer to the dimensionless transmembrane voltage and the slow current gate, respectively. The rest state of the membrane corresponds to $E = 0$ and $n = 0$. γ is a constant describing the speed of propagation of disturbances in E, while τ_E and τ_n set the time scales of the dynamics in E and n, respectively. The functions $f(E,n)$ and $g(E,n)$ are given by

$$f(E,n) = -E + [E^* - \mathcal{D}(n)][1 - \tanh(E - E_h)]\frac{E^2}{2}, \tag{3}$$

$$g(E,n) = \mathcal{R}(n)\theta(E - E_n) - [1 - \theta(E - E_n)]n, \tag{4}$$

where θ is the Heavyside step function and E^*, E_n, and E_h are constants. The restitution function, $\mathcal{R}(n)$, and the dispersion function, $\mathcal{D}(n)$, need to be defined to fully describe the behavior of the model. Restitution refers to the relationship between the diastolic interval—the interval between two subsequent action potentials—and the next action potential duration. Dispersion refers to the dependence of the speed of the front end of a pulse or action potential on the preceding diastolic interval. The functions we use are the same as in Ref. [30], and are given by

$$\mathcal{R}(n) = \frac{1 - [1 - e^{-\mathrm{Re}}]n}{1 - e^{-\mathrm{Re}}}, \tag{5}$$

$$\mathcal{D}(n) = n^M, \tag{6}$$

with parameters Re and M. See Ref. [30] for a detailed discussion of the underlying assumptions and the different parameters. Table I summarizes the parameter values we used in this study. The only parameter that is significantly different from the value given in Ref. [30] was τ_n. It was decreased from 250 ms to 15 ms in order to make the model weakly excitable and generate spirals with one SDL as observed first in Ref. [28]. We obtain qualitatively equivalent results if we increase τ_e instead. The control parameter in this study is Re,

TABLE I. Values of the model parameters (see text for details) used in this study.

τ_e	2.5	ms
τ_n	15	ms
M	4.3	
Re	1.04 to 1.15	
γ	0.0011	$\mathrm{cm}^2/\mathrm{ms}$
E_n	1.0	
E_h	3.0	
E^*	1.5415	

which controls the steepness of the restitution curve. Increasing Re makes the tissue more susceptible to alternans, however increasing it too far makes spirals unstable. While this model is clearly a simplified description of the dynamics of cardiac tissue, it allows for precise, long-term computer simulations [31] that are not feasible in many realistic electrophysiological models [32,33]. For our numerical simulations, we consider two-dimensional tissue on circular domains with no-flux boundaries as well as on rectangular domains with periodic boundaries. In the former case, the focus is on single spirals while the latter is better suited for studying multiple spirals.

III. RESULTS

Spirals were initialized by generating a plane wave, then resetting half of the wave's voltage E to zero. Initially, single spirals were simulated on circular tissues at varying Re values. Focusing on Re values in the interval [1.02,1.16], we found that normal period-one spirals become unstable giving rise to period-two spirals with single SDLs at $\mathrm{Re} \approx 1.0525$. At $\mathrm{Re} \approx 1.125$, the medium begins to continuously create and annihilate SDLs similar to the turbulent SDL regime observed in models of complex-oscillatory media [27]. Increasing Re further, breakup of period-two spirals occurs at $\mathrm{Re} \approx 1.1475$. Examples of the three main regimes can be seen in Fig. 1, while plots of the spiral period and action potential duration (APD) as a function of Re can be seen in Fig. 2.

Periodic alternations in action potential duration indicative of alternans are clearly visible in Fig. 1(b) if one follows successive wave fronts out radially from the center of the spiral. This is further highlighted by Fig. 1(d), which shows a space-time plot of the voltage along the cut indicated in Fig. 1(b). Because the spiral wave is one continuous entity, there must be a transition from short to long action potentials or vice versa at certain points on the wavefront at any given moment in time. Thus, these points do not show alternans but exhibit period-one dynamics. The set of all these points constitutes the SDLs. In Fig. 1(b), by looking at where the wavefronts change thickness, a single SDL can be observed pointing down.

In order to detect and visualize SDLs, points in the medium where these period-one dynamics are present need to be identified. There are multiple ways this can be done [10,28]. The method used in the experiments on cardiac tissue [10] involves evaluating the following integral,

$$\Delta(\vec{x},t) = \frac{1}{\tau}\int_0^\tau |E(\vec{x},t+t') - E(\vec{x},t+\tau+t')|dt'. \tag{7}$$

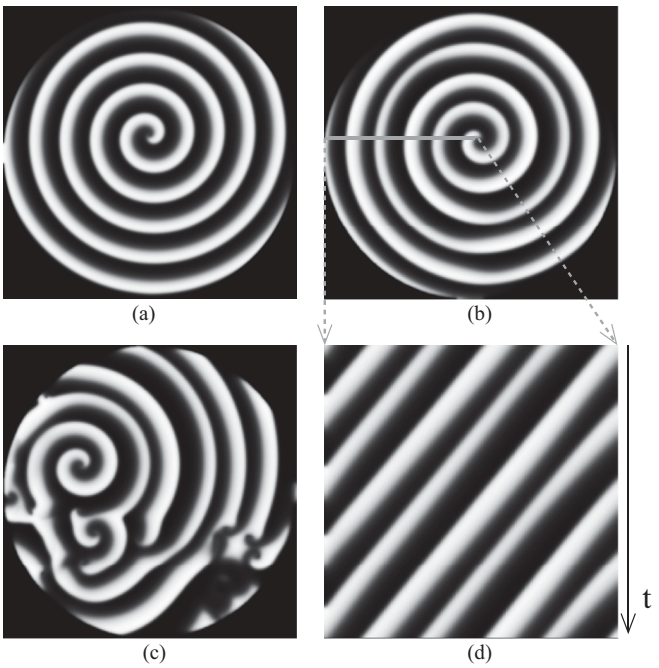

FIG. 1. Snapshots of the voltage field for spirals in three regimes relevant to this study: (a) Re < 1.05, (b) $1.05 <$ Re < 1.125, and (c) Re > 1.15. These images were taken of circular domains with a radius of 2.62 cm and a no-flux boundary. (d) shows a space-time plot along the indicated radial cut (thick line) from the spiral core in (b), clearly exhibiting alternans.

Here, τ refers to the duration of a single period-one oscillation, and locations where $\Delta(\vec{x},t)$ evaluates to zero lie on the SDL. While it is computationally expensive, this method allows one to identify SDLs continuously in time provided that they do not move too fast.

In contrast, the method typically used in the context of alternans (see, for example, Refs. [13,28]) is effectively based on a comoving reference frame attached to the wavefront or

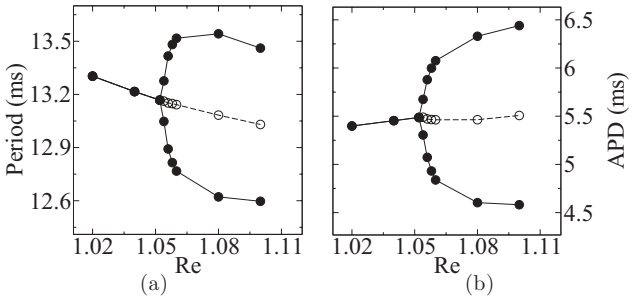

FIG. 2. (a) Average spiral rotation period, and (b) the average action potential duration[a], as functions of Re. After the period doubling, both plots contain two branches, indicating the period-two behavior of the spiral. The dashed line in the middle is an *average* of the two branches. For the spiral rotation period in (a), this average corresponds to *half* of the new period. For both spiral rotation period and APD, each data point corresponds to a numerical estimate of the asymptotic long-time average sufficiently far away from the spiral core.

[a]For this study, APD is defined as the length of time $E \geqslant 2$ as a wavefront moves through.

action potential such that the evolution of SDLs can only be observed in discrete time steps of length τ. Specifically, a local beat number $n(\vec{x},t)$ is introduced. It is set to zero everywhere in the medium initially and then incremented by one every time an action potential passes though. To identify SDLs or nodal lines, the following equation is evaluated:

$$a(\vec{x},t) = (-1)^{n_c(t)}[D(\vec{x},n_c(t)) - D(\vec{x},n_c(t)-1)]. \quad (8)$$

Here, $D(\vec{x},n)$ is the local APD corresponding to the nth beat and n_c is defined as the largest common beat number to have been recorded everywhere in the medium, $n_c(t) \equiv \min_{\vec{x}} n(\vec{x},t)$. SDLs are found to be the points where $a(\vec{x},t) = 0$. While this method has been very helpful to characterize alternans in paced cables and pinned spirals, it is not well suited to deal with moving spiral cores since the motion can significantly alter the beat numbers close to the core [34]. Moreover, the method is computationally expensive for the system sizes we consider here since one has to store the local APDs for a large number of beat numbers.

To avoid these issues and to have a more continuous picture of the time evolution of SDLs similar to the method based on Eq. (7), we propose a modified version of the above method. Specifically, we modify Eq. (8) and define $\tilde{a}$ as

$$\tilde{a}(\vec{x},t) = |D[\vec{x},n(\vec{x},t)] - D[\vec{x},n(\vec{x},t)-1]|. \quad (9)$$

As before, points where $\tilde{a}(\vec{x},t) = 0$ are part of the SDL. Unlike the method used in Ref. [28], this compares the APD for two successive wavefronts without regard to common beat number. This makes the method faster and simpler computationally than the others. However, it introduces slight discontinuities into the SDL similar to the method based on Eq. (7) [see Fig. 3(d)]. This is because in a single instant, each wavefront is tracing out a slightly different SDL due to spiral core motion. Since in our case the SDL does not move significantly over the time scale of a few spiral rotations, these discontinuities do not interfere with the overall shape or orientation of the SDL. Images generated using different SDL detection methods (including the one used for this study) can be seen in Fig. 3. Each method shows the same SDL pointing in the same direction. Note that all results presented in the following do not depend on the specific method used to identify SDLs.

A. Morphology of SDLs

Unlike the strongly curved SDLs observed in the parameter regime of normal excitability [13,28], the SDLs for weakly excitable parameter regimes studied here are nearly straight as Fig. 3 shows. While we chose this particular regime to mimic the observation of single SDLs attached to spiral cores in rat heart tissue cultures [10] as discussed above, they also found SDLs to be rather straight in the experiments. Thus, the model we study can successfully reproduce this feature as well.

It is known from Ref. [13] that models of cardiac tissue with supernormal conduction can result in stable concordant alternans in arbitrarily long-paced one-dimensional cables and straight SDLs in two-dimensional tissue, while normal conduction promotes discordant alternans and curved SDLs. This is quite consistent with what we find for the model studied here. In the parameter regime of normal excitability, the model exhibits normal conduction [30] and curved SDLs

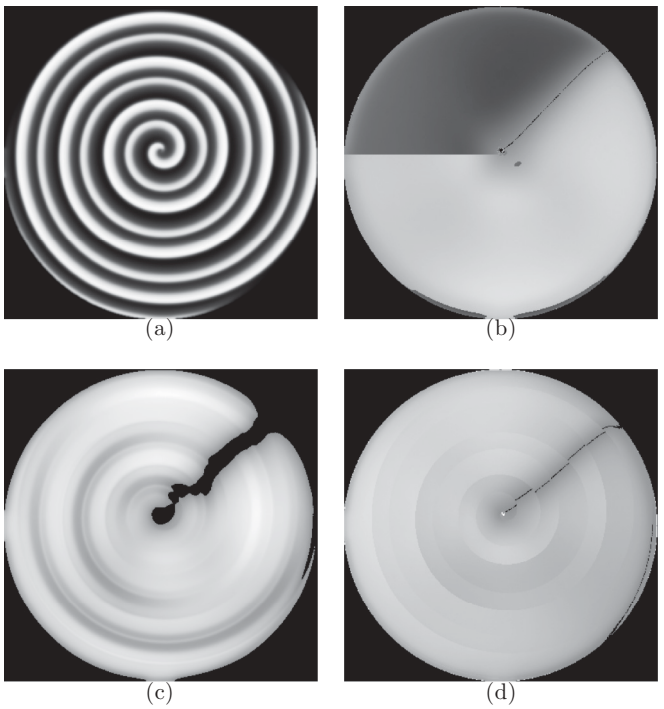

FIG. 3. (a) Dimensionless voltage, (b) the associated SDL detected using the method described in Ref. [28], (c) the method used in Ref. [10], and (d) the method used in this study.[a] The images were taken on a circular tissue with a radius of 5.24 cm and a no-flux boundary.

[a]The images seen in Figs. 3(b), 3(c), and 3(d) have had a nonlinear map applied to them, enhancing the contrast between the SDL and the rest of the image.

[28]. Changing the parameter τ_n to get into the regime of low excitability as we do here, however, changes the dispersion relation. In Fig. 4 we plot the conduction velocity of a single stable pulse in a one-dimensional (1D) system with periodic boundary conditions, corresponding to a ring configuration, for varying system sizes. For each system

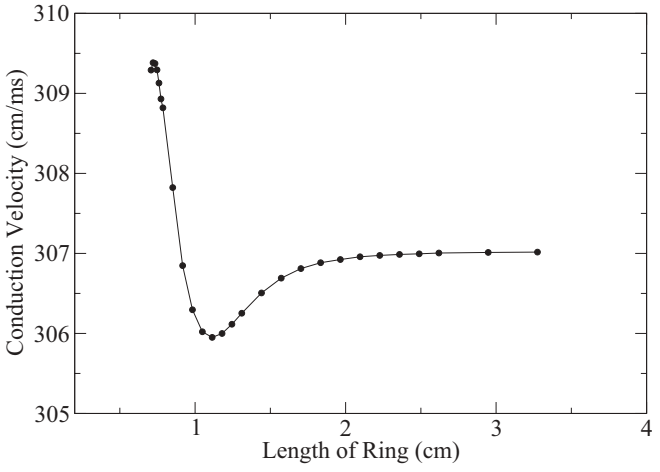

FIG. 4. Conduction velocity of a single stable pulse or action potential traveling on a ring with Re = 1.08 as a function of ring length. The behavior is qualitatively the same for all Re we considered ($1.02 \leqslant \mathrm{Re} \leqslant 1.16$).

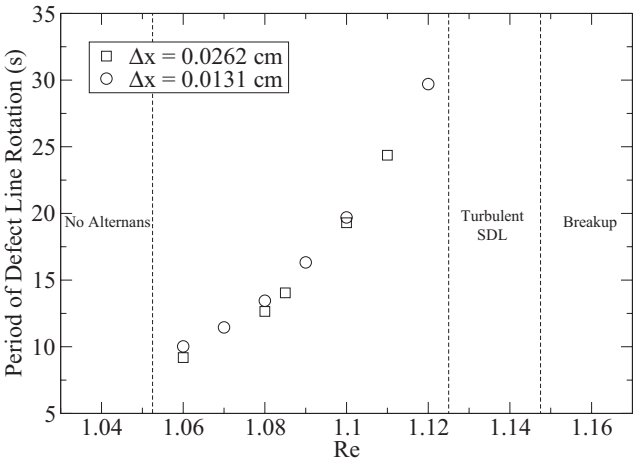

FIG. 5. Period of rotation of a single SDL attached to a free spiral in a circular domain with diameter 10.48 cm as a function of Re. For low Re values, no alternans are present. After the appearance of alternans, increasing Re increases the period of rotation. This continues until a point where SDLs start to appear and disappear constantly (turbulent SDLs). For even larger Re, the spiral simply breaks up. The variation with the spatial resolution, Δx, used for the numerical integration gives a rough estimate of the uncertainties.

size, the conduction velocity corresponds to the numerically measured asymptotic long-term average over time scales of thousands of pulse trips around the ring. While the conduction velocity is monotonically increasing corresponding to normal conduction for sufficiently long lengths, clear deviations occur for small ring lengths: The conduction velocity has a maximum at very short lengths. This should lead to stable pulse pairs and, thus, stable concordant alternans in arbitrarily long-paced one-dimensional cables as for supernormal conduction [13] but only if the pulses or action potentials are initially sufficiently close. We have confirmed this by direct numerical simulations (not shown). Thus, this behavior is consistent with the straight SDLs we see providing further evidence for a direct connection between stable concordant alternans in paced cables and straight SDLs in two-dimensional tissue. Also corroborating this observation are the results of Ref. [29], where it was found that for an effective spiral model, nonmonotonic wave dispersion as seen here results in spirals with one straight SDL.

B. Dynamics of SDLs

Focusing on the regime where a single SDL is attached to the spiral core ($1.05 \leqslant \mathrm{Re} \leqslant 1.125$), we observe that the SDL rotates slowly over time in the same direction as and at a much lower frequency than the spiral rotation. This is again in agreement with the experimental results of Ref. [10], where some spirals were found to posses rotating SDLs. As seen in Fig. 5 , the SDL rotational period increases monotonically with Re. The values shown in Fig. 5 seem to be independent of the system size, as long as the system is sufficiently large [35]. This trend continues until $\mathrm{Re} > 1.12$ where SDLs start to be spontaneously created and annihilated, mostly at boundary of the system but also inside the bulk. These additional SDLs then frequently connect and reconnect to the core. This turbulent SDL behavior is similar to what has been observed

for complex-oscillatory media [19,27]. The turbulent behavior becomes more pronounced with increasing Re.

C. Spiral core motion

To quantify the motion of the spiral core, we use its definition as a phase singularity in terms of the concept of topological charge [36–38]. Topological charge is defined as

$$q(\vec{x},t) = \frac{1}{2\pi} \lim_{R\to 0} \oint_{|\vec{x}'-\vec{x}|=R} \vec{\nabla}'\phi(\vec{x}',t) \cdot d\vec{l}', \qquad (10)$$

where $\phi(\vec{x},t)$ is the phase field. In our case, the local phase can be defined as

$$\phi(\vec{x},t) = \arctan\left(\frac{n(\vec{x},t) - n_0}{E(\vec{x},t) - E_0}\right). \qquad (11)$$

Here, (E_0,n_0) is a point inside the local limit cycles in phase space. We chose (1.2, 0.9). If the above integral is taken around a single-armed spiral core, $q(\vec{x},t)$ will evaluate to either 1 or -1. The sign refers to the spiral direction, while the absolute value refers to the number of spiral arms. If it is not taken around a core, $q(\vec{x},t) = 0$. Evaluating $q(\vec{x},t)$ numerically for all points of the discrete lattice allows one to identify the location of spiral cores over time and construct their trajectories.

In the regime where no alternans or SDLs are present, the spiral core moves on a small circle with a frequency identical to the spiral rotation frequency as expected. This is shown in Fig. 6(a). The transition to alternans, however, seems to coincide with a meandering transition introducing a second frequency. Figure 6(b) shows a plot of the core trajectory for Re = 1.08. The small orbits seen in the absence of alternans are still present, though a slower rotation is observed on top of that leading to inward petals. The period of this slower rotation is *equal* to the SDL rotation period. Because of this, it appears as though this slow rotation of the core is directly related to the rotation of the SDL, which has a finite periodicity at onset (see Fig. 5). This behavior suggests that the normal form proposed in Ref. [26]—identical to the one for the standard meandering transition—characterizes the spiral transition to alternans. Yet, in contrast to models of complex-oscillatory media, the transition itself does not seem to be a resonant 2 : 1 Hopf bifurcation but rather a nonresonant one since the former would lead to a straight drift of the core [26].

The two frequencies capture the most prominent features of core motion, but they are not sufficient to fully characterize the motion, at least away from onset. There also appear to be harmonics in the core motion with a period of about eight times the spiral rotation period. This is seen in Fig. 6(c), where running averages of different lengths were applied to a part of Fig. 6(b). The running average over one spiral rotation eliminates the smaller circles corresponding to the highest frequency motion, but leaves a trajectory that still loops around on relatively short time scales. These loops disappear only when a running average over eight times the spiral rotation frequency is applied. These harmonics do not affect the motion over large time scales.

As one would expect, the radius of the circle related to the second frequency increases with Re. However, this increase in radius is not completely due to the increase in the rotation period of the SDL. As seen in Fig. 7, the associated speed increases monotonically with Re as well. It is the combination of variable SDL rotation period and drift speed that modifies the size of the circles traced by the moving core. The confluence of these two phenomena make the drift not as apparent for Re values close to the onset of alternans and does not allow us to test the hypothesis of a nonresonant Hopf bifurcation more precisely.

The slow drift of a spiral core correlating with an SDL has been observed before in complex-oscillatory media [27]. While the core speed also increased monotonically from onset, the angle between the direction of the drift and the orientation of the single SDL decreased monotonically with the control parameter from 180 to 90 degrees. Surprisingly, the opposite behavior is seen for the model we study here. The instantaneous direction of the core drift increases monotoni-

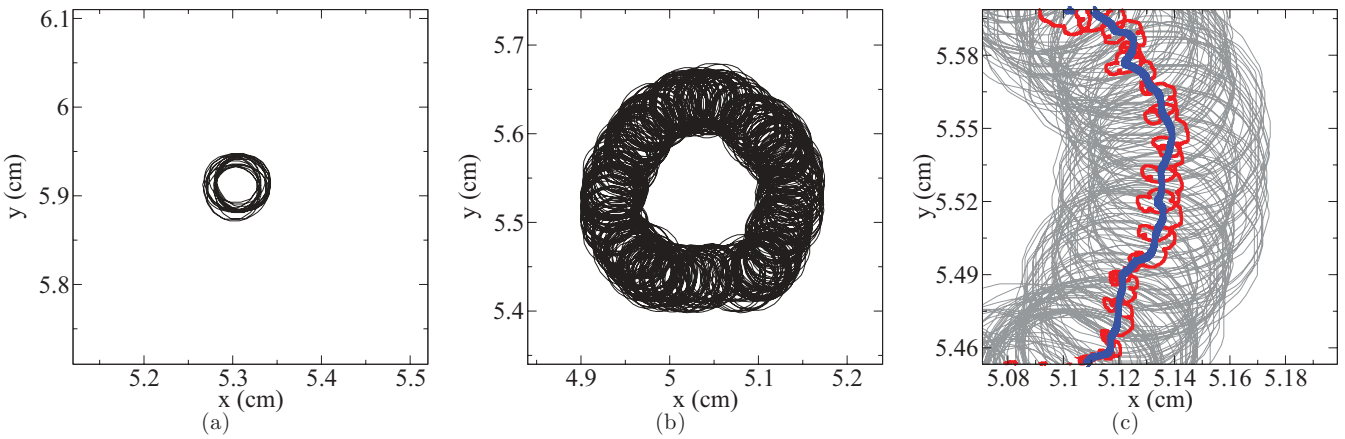

FIG. 6. (Color online) Spiral core trajectories for (a) Re = 1.02 over 493 ms, (b) Re = 1.08 over 13493 ms, and (c) a zoomed in portion of (b). Both of the core trajectories have had running averages applied over 6.25 ms in order to smooth out the trajectories, while (c) has had different running averages applied. The red (light gray) trajectory seen in (c) is the result of a running average of 25 ms (one spiral rotation), while the blue (dark gray) trajectory is the result of a running average of 200 ms (eight spiral rotations). For Re = 1.02, alternans have not yet set in, the only motion present is a circular orbit. In the alternans regime for Re = 1.08, a slowly rotating SDL is present introducing a second frequency and causing the core to exhibit inward petals.

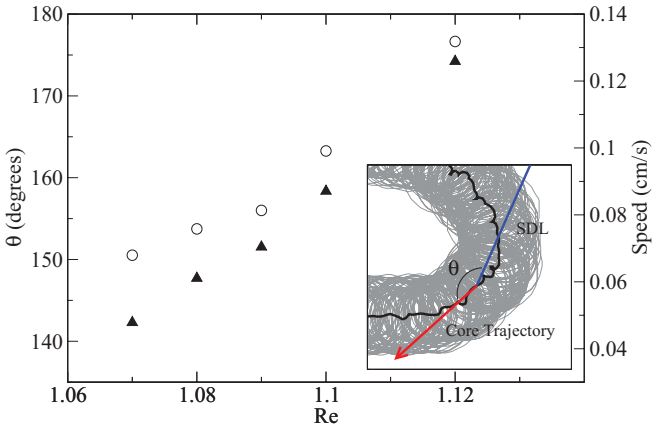

FIG. 7. (Color online) Drift speed (solid triangles) and the angle between the direction of the drift and the orientation of the SDL, θ (open circles), as functions of Re. For Re < 1.07 numerical accuracy is insufficient to obtain a clear drift trajectory, and subsequently neither a drift velocity or a drift-SDL angle could be measured for Re $= 1.06$.

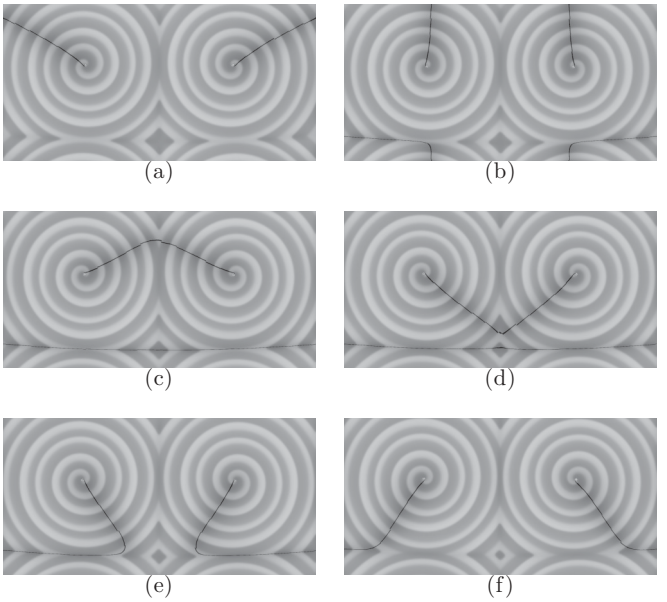

FIG. 8. Images of the voltage field with SDLs overlaid for two spirals in a periodic tissue of size 20.96 cm by 10.48 cm and Re $=$ 1.08. Images were taken at (a) 3450 ms, (b) 5750 ms, (c) 7950 ms, (d) 10550 ms, (e) 11100 ms, and (f) 13650 ms, respectively. The SDLs of each spiral both rotate, and are connected to each other at all times. Notice also how another SDL disconnects and lies on the shock line for part of the rotation.

cally with Re, approaching 180 degrees close to breakup, see Fig. 7.

The core motion undergoes another transition for Re $>$ 1.12, as the system enters the turbulent SDL regime. As mentioned above, in this regime SDLs spontaneously appear and disappear. These new SDLs frequently connect with each other and with the spiral core, strongly influencing the motion of the core. The connection and reconnection of SDLs to the core occur rapidly such that only a single SDL is connected to the core for extended periods of time. As in the nonturbulent regime, the orientation of the SDL determines the direction of the slow core drift. Other SDLs present either form closed loops detached from any spiral core, often called bubbles, or are attached to the boundary with both ends. During the time intervals between subsequent reconnections to the core, the attached SDL moves rather erratically back and forth over short distances but does not rotate. This leads to the core exhibiting almost straight line motion over such a period, with the drift direction at an angle of about 180 degrees with respect to the SDL. In addition to this angle, the speed of the core drift is also consistent with the behavior directly before onset of turbulent SDLs. For increasing Re, the system becomes more turbulent and reconnection events occur faster leading to more frequent changes in the direction of the core motion making it effectively diffusionlike.

D. Multispiral patterns

To test to which extent the dynamics of single spirals with attached SDL described above carries over to the case of multiple spirals, which are typical for sufficiently large systems and have been observed in the experiments on heart tissue [10], we focus on spiral pairs first. In the nonturbulent regime of alternans, both spiral cores are connected by an SDL. We find that provided that the initial distance between the two spirals is sufficiently large, the SDLs rotate with the same period as in the single spiral case and the rotation direction is also linked to the rotation direction of the spiral. A typical rotation is seen in Fig. 8 for periodic boundary conditions. Close to the spiral cores the SDLs are almost straight as before, yet they bend, sometimes dramatically, close to the shock lines (locations where different wavefronts meet and annihilate) separating the spirals. In particular, the SDL periodically splits into two such that the additional SDL lies completely on one of the shock lines before they reconnect later. In addition to the rotation of the SDL, the motion of the spiral cores is also analogous to the case of a single spiral.

The case of two spirals also provides additional evidence that the direction of the spiral core motion is determined by the attached SDL. Specifically, if the two spirals are sufficiently close but not too close [39], the connecting SDL does *not* rotate and the cores drift apart with a constant direction and speed as expected based on the single-spiral case for the given Re value. Once their separation is sufficiently large, the SDLs start rotating and the spiral cores meander as described above.

In situations with multiple spirals, many of the features described above survive. Figure 9 shows an example of the dynamics for such a multispiral pattern in the nonturbulent alternans regime for periodic boundary conditions. Spirals have a strong tendency to be grouped in pairs, mostly of opposite orientation or sign, connected by an SDL. Due to the periodic boundary conditions, there must be an equal number of "positive" (clockwise) and "negative" (counterclockwise) spirals [40]. Just as in the spiral-pair case, the SDLs are seen to be straight close to the spiral cores, but bend dramatically near shock lines. The SDLs then lie along these shock

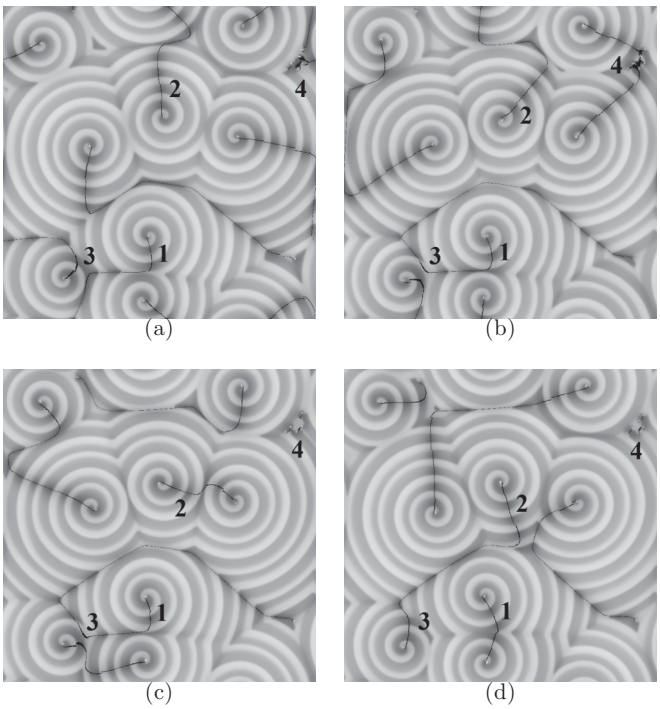

FIG. 9. Snapshots the voltage field with SDLs overlaid from a simulation of many spirals with Re = 1.08. The simulation was run on a square periodic tissue of length 20.96 cm. Snapshots show (1) nonrotation of some SDLs, (2) rotation of others, and (3) reconnection between SDLs. (4) Four tiny spirals can be seen inside the shock lines in the upper right corners of the images. Snapshots were taken at times (a) 20 s, (b) 22 s, (c) 24 s, and (d) 26 s.

lines before bending again to connect straight to another core.

In Fig. 9, some SDLs are seen to be rotating, while others are frozen. This coexistence is exactly what has been observed in rat heart tissue cultures [10]. The cores with rotating SDLs are typically farther away from shock lines than the cores with nonrotating SDLs. This matches the results seen in the spiral-pair system. The core motion also follows the exact same behavior as in the single- and double-spiral cases: The cores perform circular motion with an additional drift in a direction determined by the SDL orientation. In the case of nonrotating SDLs, this causes the cores to move away from the shock line, similar to the case of two spirals sufficiently close together. For rotating SDLs, the core meanders.

Inevitably, the pattern rearranges over time due to the rotation of the SDLs and the associated motion of the spiral cores. Reconnections are seen to occur between SDLs such that cores exchange partners frequently. A specific example of this is labeled as 3 in Fig. 9. Another feature of these multispiral patterns is the presence of spirals with wave fields that are confined to tiny areas. These "passive" spirals still have SDLs, which can attach to other spiral cores. However, their cores move under different dynamics than the larger spirals resembling passively advected entities.

Varying Re has the same effect as in the case of single spirals. Higher Re values lead to faster SDL rotation and higher drift speeds as well as larger angles between the direction of the drift and the SDL. In the turbulent SDL regime for $\mathrm{Re} > 1.2$, the spontaneous creation and annihilation of SDLs leads to more frequent reconnections and increasingly erratic motion of SDLs and spiral cores. Spiral cores with three SDLs attached to them for extended periods of time also occur more frequently.

IV. DISCUSSION

Despite the fact that the model of cardiac tissue we study here is very simple and rather a conceptual model, it reproduces all the major observations in experiments on *in vitro* tissue cultures of neonatal rat ventricular myocytes [10]: In the alternans regime, single and almost straight SDLs are connected to spiral cores. Stationary SDLs coexist with rotating SDLs and the latter rotate very slowly in the same direction as the rotation of the spiral wave. Our findings suggest that this coexistence is due to the interaction of multiple spirals. While no spiral core motion has been reported in the experiments, this does not mean that such motion is absent. In particular, our analysis shows that the motion can be very minimal and barely detectable especially close to onset of the alternans regime. Our model also provides evidence that nonmonotonic conduction is essential to reproduce the experimental findings, supporting other model studies [13,29,41]. To our best knowledge, the model studied here is currently the only one that can reproduce all the experimental features described above.

Some of the features we observe in the regime of low excitability, also hold if we chose the model parameters in the regime of normal excitability ($\tau_n = 250$ ms). Despite the fact that three fast-rotating and strongly curved SDLs are attached to a single spiral core in the alternans regime [28], simulations show that the core motion also exhibits a meandering transition to inward petals. These inward petals become more pronounced for larger values of Re indicating an increase in the speed associated with the second frequency as for low excitability. These qualitative similarities prove that low excitability and nonmonotonic conduction are not necessary conditions to observe these particular features. While our simple model study is not directly applicable to human arrhythmias, the robustness of these features indicates that they could also play a role in some cardiac arrhythmias. Certainly, much more work is necessary to establish whether this is true and, if yes, to what extent. Possible venues include studies of more realistic heart models like those in Refs. [8,13,42–44], which are still computationally tractable.

Finally, while our analysis has focused on excitable media, rotating SDLs in combination with spiral core meander have also been observed in chemical experiments of the Belousov-Zhabotinsky reaction in a regime where the underlying dynamics is complex-oscillatory [21,23]. This indicates that such a behavior is rather general and not specific to excitable media or cardiac tissue. Interestingly, in these chemical experiments the SDL motion can even undergo another Hopf bifurcation making the overall motion even more complicated—a phenomenon we do not observe here but could be observable in other models as, for example, the ones in Refs. [8,12,13,45].

ACKNOWLEDGMENTS

We thank J. Restrepo for helpful discussions related to the model and A. Scheel for helpful discussions related to the resonant Hopf bifurcation and the meandering transition. This project was financially supported by NSERC and mprime (formerly MITACS).

[1] A. Mikhailov, *Foundations of Synergetics I: Distributed Active Systems* (Springer Verlag, New York, 1994).
[2] *Chemical Waves and Patterns*, edited by R. Kapral and K. Showalter (Kluwer Academic, Dordrecht, 1995).
[3] R. C. Desai and R. Kapral, *Dynamics of Self-organized and Self-assembled Structures* (Cambridge University Press, Cambridge, 2009).
[4] M. Bär and L. Brusch, New J. Phys. **6**, 5 (2004).
[5] D. Barkley, Phys. Rev. Lett. **68**, 2090 (1992).
[6] D. Barkley, Phys. Rev. Lett. **72**, 164 (1994).
[7] B. Sandstede and A. Scheel, Phys. Rev. Lett. **86**, 171 (2001).
[8] F. H. Fenton, E. M. Cherry, H. M. Hastings, and S. J. Evans, Chaos **12**, 852 (2002).
[9] J. N. Weiss, Z. Qu, P.-S. Chen, S.-F. Lin, H. S. Karagueuzian, H. Hayashi, A. Garfinkel, and A. Karma, Circulation **112**, 1232 (2005).
[10] T. Y. Kim, S.-J. Woo, S.-M. Hawang, J. H. Hong, and K. J. Lee, Proc. Natl. Acad. Sci. USA **104**, 11639 (2007).
[11] J. J. Fox, E. Bodenschatz, and R. F. Gilmour, Phys. Rev. Lett. **89**, 138101 (2002).
[12] B. Echebarria and A. Karma, Phys. Rev. E **76**, 051911 (2007).
[13] B. Echebarria, G. Röder, H. Engel, J. Davidsen, and M. Bär, Phys. Rev. E **83**, 040902(R) (2011).
[14] J. Pastore, S. D. Girouard, K. R. Laurita, F. G. Akar, and D. Rosenbaum, Circulation **99**, 1385 (1999).
[15] J. N. Weiss, A. Karma, Y. Shiferaw, P.-S. Chen, A. Garfinkel, and Z. Qu, Circ. Res. **112**, 1232 (2006).
[16] A. Karma and R. F. Gilmour, Phys. Today **60**, 51 (2007).
[17] A. Goryachev and R. Kapral, Phys. Rev. Lett. **76**, 1619 (1996).
[18] A. Goryachev and R. Kapral, Phys. Rev. E **54**, 5469 (1996).
[19] A. Goryachev, R. Kapral, and H. Chaté, Int. J. Bifurcation Chaos Appl. Sci. Eng. **10**, 1537 (2000).
[20] J.-S. Park and K. J. Lee, Phys. Rev. Lett. **83**, 5393 (1999).
[21] J.-S. Park and K. J. Lee, Phys. Rev. Lett. **88**, 224501 (2002).
[22] J.-S. Park, S. J. Woo, and K. J. Lee, Phys. Rev. Lett. **93**, 098302 (2004).
[23] J.-S. Park and K. J. Lee, Phys. Rev. E **73**, 066219 (2006).
[24] H. Y. Guo, L. Li, H. L. Wang, and Q. Ouyang, Phys. Rev. E **69**, 056203 (2004).
[25] C. Zhang, H. Liao, and Q. Ouyang, J. Phys. Chem. B **110**, 7508 (2006).
[26] B. Sandstede and A. Scheel, SIAM J. App. Dyn. Syst. **6**, 494 (2007).
[27] J. Davidsen, R. Erichsen, R. Kapral, and H. Chaté, Phys. Rev. Lett. **93**, 018305 (2004).
[28] J. G. Restrepo and A. Karma, Phys. Rev. E **79**, 030906 (2009).
[29] O. Kwon, T. Y. Kim, and K. J. Lee, Phys. Rev. E **82**, 046213 (2010).
[30] A. Karma, Chaos **4**, 461 (1994).
[31] The equations were integrated using a simple forward Euler scheme with a nine-point Laplacian with $\Delta t = 0.025$ ms and $\Delta x = 0.0131$ cm.
[32] R. H. Clayton and A. V. Panfilov, Prog. Biophys. Mol. Biol. **96**, 19 (2008).
[33] R. Clayton, O. Bernus, E. Cherry, H. Dierckx, F. Fenton, L. Mirabella, A. Panfilov, F. Sachse, G. Seemann, and H. Zhang, Prog. Biophys. Mol. Biol. **104**, 22 (2011).
[34] One could circumvent this problem by ignoring the area in which the core moves for computing the largest common beat number. However, this would prevent one from identifying the structure of the SDLs or nodal lines close to the core.
[35] Significant finite-size deviations occur for diameters less than 5.24 cm.
[36] N. Mermin, Rev. Mod. Phys. **51**, 591 (1979).
[37] J. Davidsen and R. Kapral, Phys. Rev. Lett. **91**, 058303 (2003).
[38] G. St-Yves and J. Davidsen, J. Chem. Phys. **133**, 044909 (2010).
[39] If the spirals are too close, they can form a bound pair and behave as a single compound entity following a different dynamics altogether.
[40] J. Davidsen, L. Glass, and R. Kapral, Phys. Rev. E **70**, 056203 (2004).
[41] A. Goryachev and R. Kapral, Int. J. Bifurcation Chaos Appl. Sci. Eng. **9**, 2243 (1999).
[42] C. C. Mitchell and D. G. Schaeffer, Bull. Math. Biol. **65**, 767 (1999).
[43] O. Bernus, R. Wilders, C. W. Zemlin, H. Verschelde, and A. V. Panilov, Am. J. Physiol.: Heart Circ. Physiol. **282**, H2296 (2002).
[44] A. Bueno-Orovio, E. M. Cherry, and F. H. Fenton, J. Theor. Biol. **253**, 544 (2008).
[45] B. Echebarria and A. Karma, Eur. Phys. J.: Special Topics **46**, 217 (2007).